Localization of charge carriers in the normal state of underdoped $Bi_{2+x}Sr_{2-x}CuO_{6+\delta}$

Huiqian Luo[1,*] and Hai-Hu Wen[2]

[1]*Beijing National Laboratory for Condensed Matter Physics, Institute of Physics, Chinese Academy of Sciences, Beijing 100190, China*

[2]*Center for Superconducting Physics and Materials, National Laboratory for Solid Microstructures and Physics Department, Nanjing University, Nanjing 210093, China*

(Received 1 August 2013; revised manuscript received 1 January 2014; published 14 January 2014)

We report the transport results of underdoped $Bi_{2+x}Sr_{2-x}CuO_{6+\delta}$ ($0.05 \leqslant x \leqslant 0.40$) single crystals. A close relationship between the upturn of in-plane resistivity [$\rho_{ab}(T)$] and the sign of magnetoresistance in the normal state upon Bi substitutions is found. Combining the results of the field and angular dependence of magnetoresistance, the model fitting of $\rho_{ab}(T)$, as well as the Hall coefficient results, we suggest a crossover from weak to strong localization of charge carriers in the underdoped $Bi_{2+x}Sr_{2-x}CuO_{6+\delta}$, which may be responsible for the rather narrow superconducting dome in this system.

DOI: 10.1103/PhysRevB.89.024506 PACS number(s): 74.72.Gh, 74.25.F−, 71.10.Hf, 72.15.Rn

I. INTRODUCTION

The exotic transport properties in the normal state of high transition temperature superconductors (HTSCs) have been the subjects of considerable theoretical attentions and sources of fascinating experimental investigations [1]. In contrast to the clear pictures in the overdoped regime, the transport properties in the underdoped side are far from well understood due to the complex competing behaviors among various orders [2,3]. Among different cuprate families, the single-layered $Bi_2Sr_{2-x}Ln_xCuO_{6+\delta}$ (Ln = La, Pr, Nd, Sm, Eu, Gd, etc.) (Ln-Bi2201) system is one of the best materials for studying the novel ground states of HTSCs, which can be achieved by either the chemical substitution outside the Cu-O planes or oxygenation within the Cu-O layers [1]. The out-of-plane substitution by Ln drives the T_c of optimal superconductivity from 35 K in La-Bi2201 to about 10 K in the pure $Bi_{2+x}Sr_{2-x}CuO_{6+\delta}$ (Bi2201) [4–9]. In the meantime, T_c also can be tuned by oxygenation in the post-annealing process [10]. The rich chemistry of the Bi2201 system offers an opportunity to elucidate the normal-state properties of HTSCs in the comparatively simple case of single-layer compounds. Especially for the pure Bi2201, the normal state at low temperatures can be easily reached by applying a magnetic field large enough to totally suppress the superconductivity at the measured temperatures [11] due to its rather low upper critical field (less than 25 T at 0 K) [7,8]. In the past 20 years, many classic transport researches have been done in the La-Bi2201 system, establishing some important pictures such as the non-Fermi-liquid nature of cuprates [12–17]. However, the results of the pure Bi2201 system mainly focus on the high magnetic field effects on the transport properties of the moderate doped samples [7,8,18–24]. The transport behaviors of the underdoped samples under low fields, especially for the crossover between the insulating and superconducting regimes, remain to be explored.

It is well observed that for most of the underdoped cuprates, a semiconductinglike upturn in resistivity appears at the temperatures close to T_c, commonly attributed to the dilution of the charge carriers and the metal-to-insulator crossover [12–21]. Such behavior also indicates that the scattering mechanism of quasiparticles is much more complex when the temperature approaches to T_c in the underdoped regime [25–27]. In the Ln-Bi2201 system, the superconducting dome, namely, the bell shaped, is distorted and much narrower than those in $YBa_2Cu_3O_{7-\delta}$ (Y123) and $La_{2-x}M_xCuO_4$ (M = Sr, Ca, Ba, etc.) (La214) systems [10,28–31]. Recent angle-resolved photoemission spectroscopy (ARPES) measurements on our Bi2201 crystals also suggest that the pseudogap in the underdoped regime evolves into a large soft Coulomb gap when the system approaches the insulating phase, which pushes the superconducting threshold to higher doping concentration [32]. In pursuing the understanding of the mechanism of superconductivity and the distorted phase diagram of the Bi2201 system, it is of fundamental importance to investigate the electrical transport behaviors in the normal state.

Here, we report detailed studies on the temperature, magnetic field, and angular dependence of MR and Hall coefficients in Bi2201 single crystals throughout the underdoped regime. We find a close relationship between the upturn of in-plane resistivity [$\rho_{ab}(T)$] and the behaviors of MR in the normal state of Bi2201 with different Bi-substitution content x. By comparing these results with previous works, we conclude that a crossover from weak to strong localization of charge carriers is induced by out-of-plane Bi substitution in the underdoped regime. Thus both localization effect and reduction of hole concentration contribute to the suppression of superconducting dome in Bi2201.

II. EXPERIMENTAL DETAILS

We have successfully grown high-quality $Bi_{2+x}Sr_{2-x}CuO_{6+\delta}$ ($0 \leqslant x \leqslant 0.5$) single crystals by traveling-solvent floating-zone method [9]. The high density of doping carriers for our crystals enables us to investigate the transport properties extensively in the underdoped regime. Figure 1 shows the phase diagram of our samples in the underdoped regime with Bi-substitution content ranging from $x = 0.05$ to 0.40, where the optimal $T_{c_{max}}$ in this system is about 9 K at $x = 0.05$. The bottom x axis is the hole concentration p deduced from ARPES measurements [32] by integrating the whole Fermi surface area in linear dependence of x: $p = 0.182 - 0.36x$. Since the Bi^{3+} substitution for

*hqluo@iphy.ac.cn

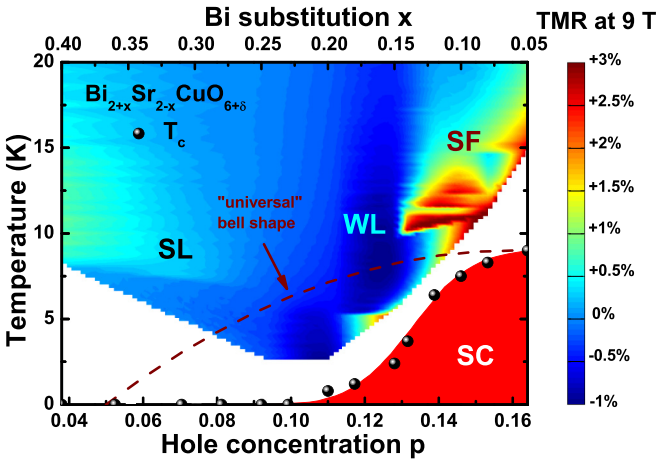

FIG. 1. (Color online) Phase diagram of our Bi2201 single crystals, where the hole concentration p is deduced from ARPES results with $p = 0.182 - 0.36x$. The solid line is the "universal" bell shape defined as $T_c/T_{c\max} = 1 - 82.6(p - 0.16)^2$, much broader than the superconducting (SC) dome of Bi2201. The gradient color is TMR at $H = 9$ T. Upon Bi substitution, the clear sign change of TMR suggests the scattering mechanism evolves from superconducting fluctuation (SF), weak localization (WL) to strong localization (SL) in the normal state.

Sr^{2+} introduces electron doping and thus reduces the hole concentration p, the system is pushed away to the underdoped side by increasing the Bi^{3+} doping, where the superconductivity is totally suppressed around $x = 0.23$. Comparing to the normalized superconducting dome of La-Bi2201 [16], the dome shape of Bi2201 is highly distorted [9,10]. Both of them are much narrower than the "universal" bell shape [31] in the form of $T_c/T_{c\max} = 1 - 82.6(p - 0.16)^2$ (the solid line in Fig. 1). Therefore the effect of the out-of-plane substitution in Bi2201 system is not the same as that of the oxygenation in the Cu-O layer. Dual effects from both the chemical disorder and the doping may play important role in the evolution of the superconductivity [4,5,33].

To study the effect of the out-of-plane substitution on the scattering mechanism of charge carries in the normal state, we have systematically performed resistivity and magnetoresistance measurements on the underdoped Bi2201 under magnetic field. The typical sizes of these single crystals are about $1 \times 2 \times 0.03$ mm^3, with the c axis oriented along the smallest dimension. Four Ohmic contacts with low resistance (about 1 Ω) on ab plane were made by silver epoxy (H20E type). The measurements were carried out on a Quantum Design Physical Property Measurement System (PPMS). A sense current $I = 1$ mA was applied to the ab plane by the standard four-probe method. In order to lower the noise, we used a rather slow sweeping rate of temperature (0.4 K/min) and magnetic field (50 Oe/s) in all measurements of MR. Here, we define transverse magnetoresistance (TMR) with $H \| c \perp I$ geometry, and longitudinal magnetoresistance (LMR) with $H \| ab \| I$ geometry. The angular dependent magnetoresistance (AMR) was also determined by rotating the sample with the angle θ between H and c from 0° to 360° in 1°/step. The Hall coefficient was measured by magnetic field scan at selected temperatures and confirmed by temperature scan under $H = \pm 9$ T. The thermal hysteresis of the temperature sensors (Cernox) and the residual contribution of the Hall effect were eliminated by applying current or field in opposite directions. All results are double checked on several crystals with the same Bi content.

III. RESULTS AND DISCUSSION

Before describing the sign change of TMR in Fig. 1 in detail, we first discuss the in-plane resistivity $\rho_{ab}(T)$ under zero field shown in Fig. 2. In the nearly optimally doped compounds with $x = 0.05$, 0.10, and 0.12, the ρ_{ab} in the normal state increases linearly up to room temperature, which represents the

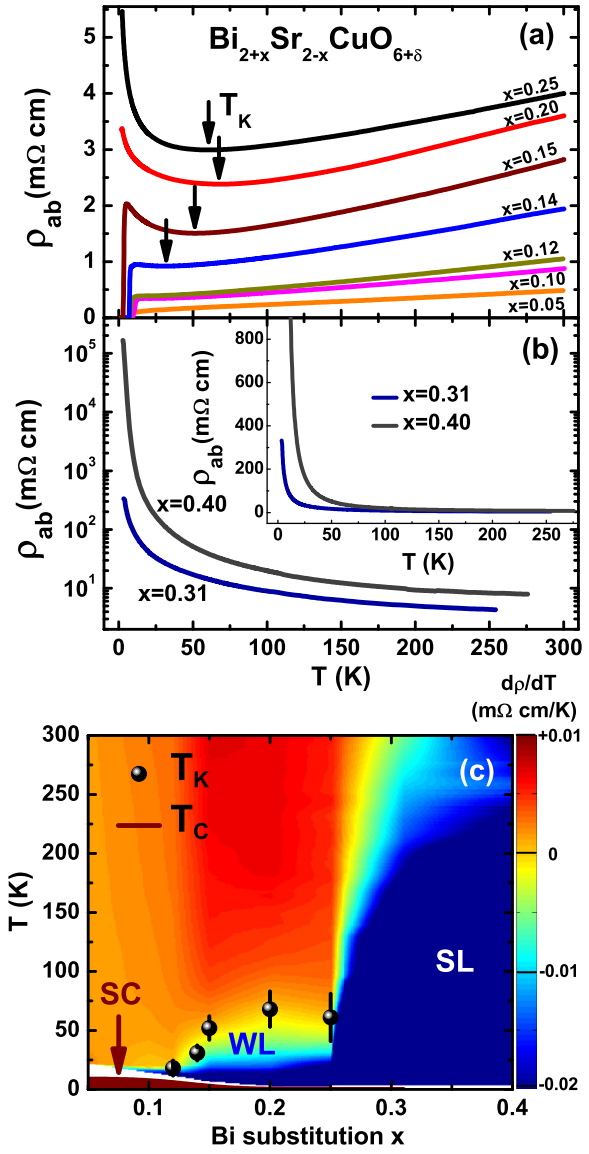

FIG. 2. (Color online) (a) Temperature dependence of in-plane resistivity $\rho_{ab}(T)$ for Bi2201 single crystals with $x = 0.05 \sim 0.25$. (b) $\rho_{ab}(T)$ for the extremely underdoped compounds with $x = 0.31$ and 0.40 both in logarithmic and linear (insert) scale. (c) Temperature and doping dependence of $d\rho_{ab}(T)/dT$, where T_K is the "kink" temperature corresponding to the sign change point of the slope of $\rho_{ab}(T)$.

non-Fermi liquid behavior in Bi2201 [1,13]. A little bit raise in $\rho_{ab}(T)$ when approaching the superconducting transition emerges in $x = 0.14$ compound and evolves into a clear upturn for $x = 0.15$, 0.20, and 0.25 [see Fig. 2(a)]. By further Bi substitution, $\rho_{ab}(T)$ gradually changes into a diverging behavior at low temperature in nonsuperconducting samples with $x = 0.31$ and 0.40, as an evidence of the superconducting-insulating zone boundary. Such semiconducting-like behavior of $\rho(T)$ is a common feature of underdoped cuprates [12–16], especially for the quasi-two-dimensional (2D) systems with single Cu-O layer [18,22]. For a qualitative comparison of the "kink" of resistivity versus Bi substitution, we plot the slope of $\rho_{ab}(T)$ in Fig. 2(c). A clear sign change of $d\rho_{ab}(T)/dT$ is found around T_K above $x = 0.12$.

It is well known that the 2D weak localization (WL) of charge carriers may induce such upturn behavior of in-plane resistivity in underdoped cuprates [25–27]. In this case, the $\rho_{ab}(T)$ in the low-temperature region just above T_c should follow this model [13,34–37]:

$$\rho(T) = a - \rho_0 \ln(T/T_0). \quad (1)$$

As shown by the green lines in Fig. 3(a), the WL-fitting captures the main features of $\rho_{ab}(T)$ in the upturn region for $x = 0.15$ and 0.20, where a clear linear zone could be found in the relation of $\rho_{ab}(T)$ versus $\ln(T)$ [insert of Fig. 3(a)]. In addition, the ARPES measurements on Bi2201 clearly show a suppression of the spectral weight ("gap") up to $\Delta \sim 0.19$ eV

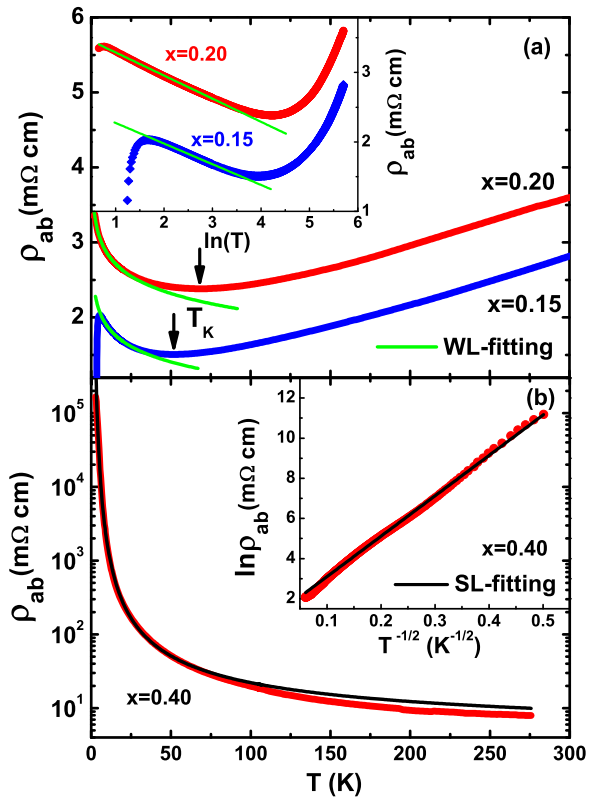

FIG. 3. (Color online) (a) WL fitting (green lines) in the upturn region for $x = 0.15$ and 0.20 by Eq. (1), where insert shows in logarithmic scale. (d) SL fitting (black lines) for $x = 0.40$ by Eq. (2), where insert shows the linear dependence of $\ln\rho_{ab}$ vs $T^{-1/2}$.

TABLE I. The model fitting parameters of $\rho_{ab}(T)$ for Bi2201 single crystals with $x = 0.15$, 0.20, and 0.40.

x	Model	ρ_0 (mΩ cm)	T_0 (K)
0.15	WL	0.30 ± 0.01	37 ± 5
0.20	WL	0.33 ± 0.01	42 ± 5
0.40	SL	2.9 ± 0.2	400 ± 10

for the $x \geqslant 0.31$ samples without clear coherent peaks [32]. By comparing with the theory of the classical Coulomb gap, it is interpreted as a soft Coulomb gap. Therefore the insulatinglike behavior at low temperature for $x = 0.40$ may be explained by the strong localization (SL) model of variable-range hopping (VRH) with a soft Coulomb gap [35,38,39]:

$$\rho = \rho_0 \exp[(T_0/T)^{1/2}]. \quad (2)$$

Here, $T_0 = e^2/\kappa\xi$ is the long-range Coulomb energy scale determined by the dielectric constant κ and the localization length ξ. We plot the fitting result in Fig. 3(b), where a linear relation also can be found for $\ln[\rho_{ab}(T)]$ versus $T^{-1/2}$ [insert of Fig. 3(b)]. The WL and SL model fitting parameters of $\rho_{ab}(T)$ are summarized in Table I. The long-range Coulomb energy scale T_0 is about 400 K, qualitatively agreeing with the visible soft gap even above 280 K in ARPES measurements [32]. One may notice the deviation at high temperatures in these fittings. Since the WL and SL models describe the scattering processes of electron-electron, electron-spin, and/or electron-impurity, these interactions manifest themselves in low-temperature range in most cases where the thermal activation is absent. Indeed, the fittings capture the main features of the upturns of $\rho_{ab}(T)$ below 50 K for $x = 0.40$ and below 25 K for $x = 0.15$ and 0.20. Therefore it suggests that a crossover from WL to SL of charge carriers happens after introducing more out-of-plane Bi substitutions, where superconductivity is totally suppressed in this doping regime. As the $x = 0.25$ and 0.31 samples are located in the crossover regime, neither the WL model nor the SL model can fully describe the $\rho_{ab}(T)$ behavior of them.

To further confirm the localization picture from the fitting results of $\rho_{ab}(T)$, we have also investigated the MR in the normal state of underdoped Bi2201. Here, MR is defined as

$$\Delta\rho_{ab}(H)/\rho_{ab}(0) = [\rho_{ab}(H) - \rho_{ab}(0)]/\rho_{ab}(0), \quad (3)$$

where H is the applied magnetic field ranging from 0.5 to 9 T. Figure 4 shows the normal state TMR under $H \| c \perp I$ for typical compounds with $x = 0.05$, 0.10, 0.12, 0.14, 0.15, 0.20, 0.25, 0.31, and 0.40. One immediately observed feature is the sign change of TMR at different doping levels. For the slightly underdoped samples with $x = 0.05$–0.14, where no obviously upturn in $\rho_{ab}(T)$ is found [see Fig. 2(a)], the normal state TMR is always positive and decays quickly as temperature increases [see Figs. 4(a)–4(d)]. Once upturn of $\rho_{ab}(T)$ shows up in $x = 0.15$ and 0.20 compounds, TMR changes sign to negative [see Figs. 4(e)–4(f)]. After reaching a maximum at certain temperature, the negative TMR also decays as temperature increases. In the samples with $x = 0.25$, $p = 0.09$, no superconductivity is found above 2 K. Most parts of TMR curves are positive with only a tiny negative TMR below 15 K and above 7 T [see Fig. 4(g)]. For the heavily doped

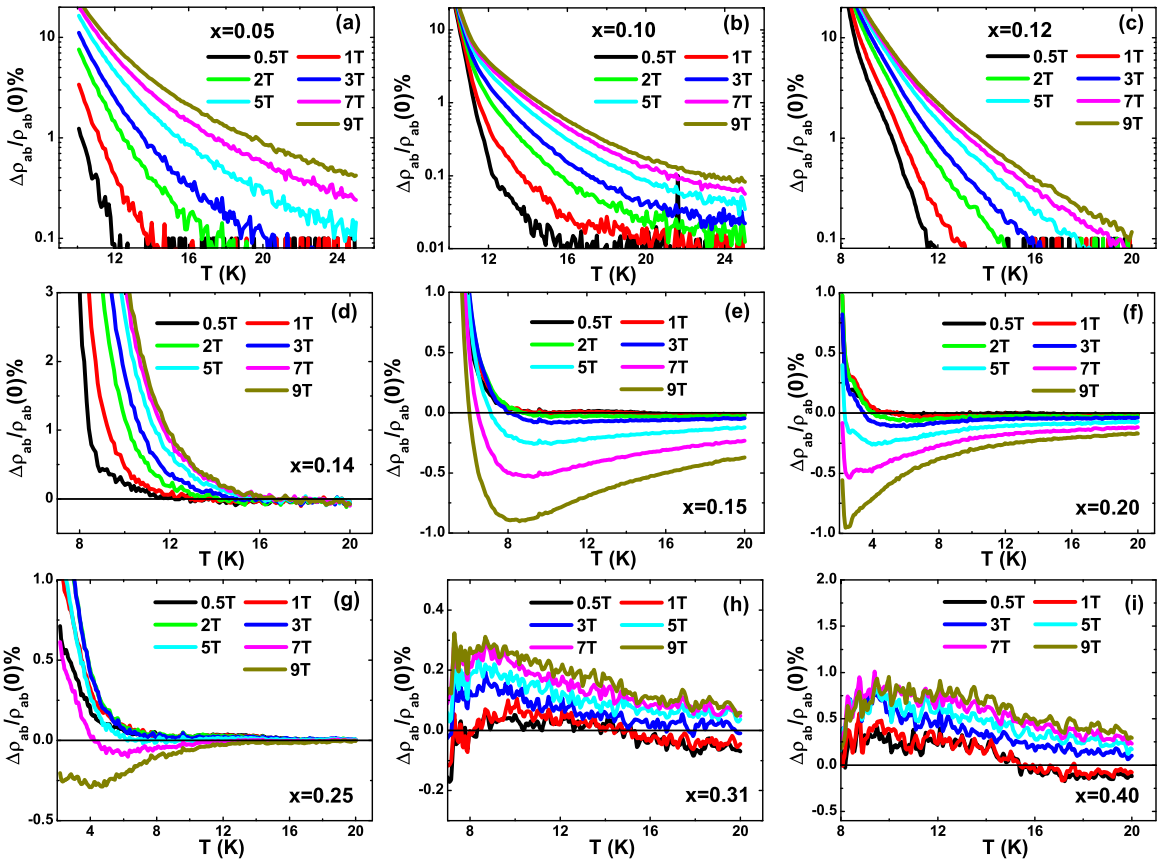

FIG. 4. (Color online) (a)–(e). The normal state TMR under $H \| c$ and $I \| ab$ for typical compounds with $x = 0.05$, 0.10, 0.12, 0.14, 0.15, 0.20, 0.25, 0.31, and 0.40.

sample with $x = 0.31$ and 0.40, the resistivity is insulatinglike at low temperatures. Although the MR appears with too many noises due to large magnitude of ρ_{ab}, it is generally positive and slightly enhanced by the magnetic field by less than 1% [see Figs. 4(h) and 4(i)].

We summarize the doping evolution of TMR at $H = 9$ T in Fig. 1 by gradient colors ranging from -1% to $+3\%$, where the blue area indicates the negative TMR. It is well known that the magnetic field destroys the cooper pairs and thus suppress the superconducting fluctuations just above T_c. Magnetic transport measurements on our Bi2201 samples have revealed large amplitude of superconducting fluctuations, which can be explained in terms of a Ginzburg-Landau approach by the introduction of a total-energy cutoff in the fluctuation spectrum [40]. Therefore the significant positive TMR in $x = 0.05$–0.14 can be simply understood as a result of the suppression of superconducting fluctuations. On the other hand, the 2D-WL theory predicts a negative MR when the spin-orbit coupling is weak [35,41]. Since the applied magnetic field could break the local interference of charge carriers and then weaken the localization effect, more delocalized charge carriers will contribute to the conductivity and lower the resistivity. When the delocalization effect from magnetic field is stronger than the suppression effect of superconducting fluctuations in the WL region, a negative MR will emerge. Such negative MR has already been observed in many cuprates [27,42,43]. For both La and Bi substituted Bi2201 systems, negative out-of-plane MR was found to be related to either the superconducting fluctuations or spin effects on the pseudogap in the normal state [19,24,44]. We also observed that a negative in-plane MR has already been found in pure Bi2201 with $T_c = 6.8$–8 K under low field, which is better to be interpreted by the interaction theory rather than the localization theory due to both $\sqrt{T}$ and $\sqrt{B}$ dependencies under a high field [23]. While in our case the hole concentration with negative in-plane MR is much lower than in the optimal doped sample with maximum $T_c = 9$ K and close to insulate zone boundary, one of the most likely mechanisms for such negative MR is the magnetic field suppression of localization effects. If the localization effect grows up, such small energy from a magnetic field is not enough to delocalize the charge carriers. Instead, for the sample close to the AFM regime, the spin order will give another positive $\gamma^{\mathrm{AF}} H^2$ contribution to MR [25,26,42]. The p of the $x = 0.40$ sample is about 0.04, which is very closed to the AFM boundary [32,45]. It is thus reasonable to have a positive MR due to the strong scattering from the spin-spin correlations. Moreover, it is usually suggested that MR has the same sign as the corresponding temperature coefficient of the resistivity $\Delta\rho_{ab}/\rho_{ab} = Q\partial \ln \rho_{ab}/\partial T$, where Q is a positive coefficient depending on the real scattering mechanism [42]. This is a phenomenal explanation for the link between the sign of MR and the curvature of $\rho_{ab}(T)$ in our samples.

We have also investigated the field dependence of MR on two typical superconducting compounds with $x = 0.12$ and 0.15. Both the TMR under $H \| c \perp I$ geometry and LMR under $H \| I \| ab$ geometry are shown in Fig. 5, where the solid

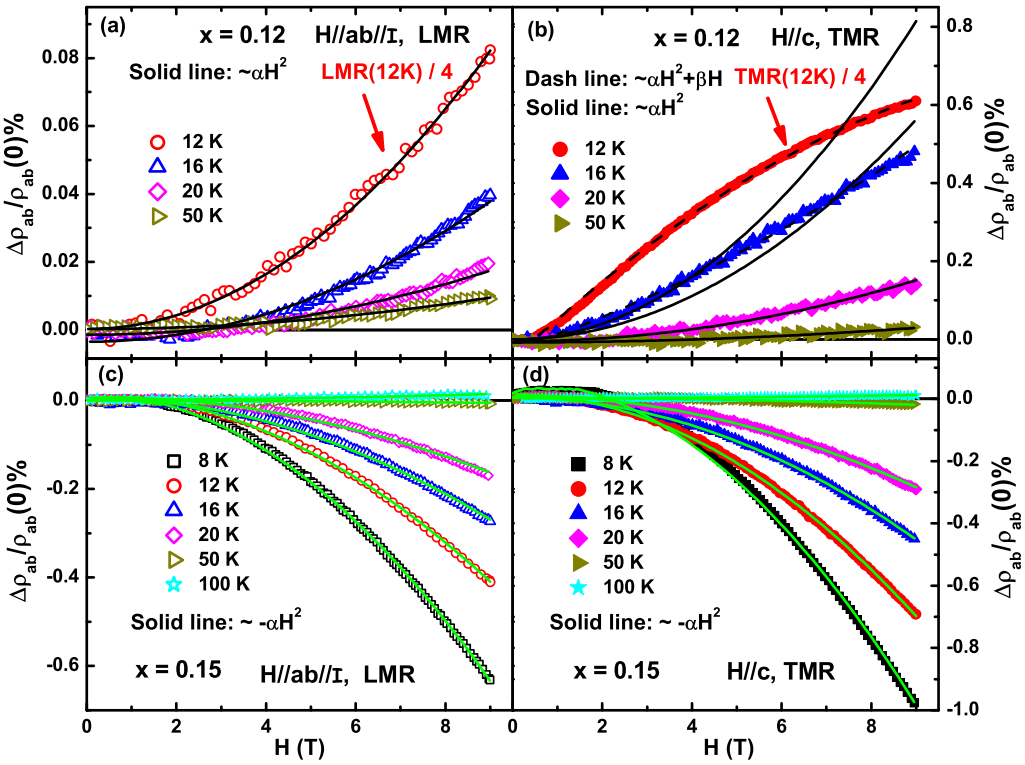

FIG. 5. (Color online) (a) and (b) The field dependence of LMR and TMR in $x = 0.12$ sample at 12, 16, 20, and 50 K, where the solid lines and dash lines are polynomial fitting curves by $\sim\alpha H^2$ and $\sim\alpha H^2 + \beta H$, respectively. (c) and (d) The field dependence of LMR and TMR in $x = 0.15$ sample at 8, 12, 16, 20, 50, and 100 K.

lines and dashed lines represent the pure square law $\sim\alpha H^2$ and quadratic law mixed with a linear term $\sim\alpha H^2 + \beta H$, respectively. Generally, both LMR and TMR almost follow the pure H^2 law except for $x = 0.12$ at 12 and 16 K, which is mixed by an additional linear term $\sim\alpha H^2 + \beta H$ [see Fig. 5(b)]. The origin of such anomalous H-linear term in the TMR just above T_c is not very clear yet [46]. It is possible due to the contribution from the scattering of flux flow [47,48]. The positive H^2 term of MR in $x = 0.12$ sample is a typical feature of the suppression of superconducting fluctuation [49]. It should be noted that the negative MR in the $x = 0.15$ sample is totally smeared above 50 K, where there is no upturn in resistivity. The Kohler's rule is violated in our MR results, resulting from the non-Fermi-liquid behaviors as shown by previous works [27,50]. Furthermore, the similar behaviors of LMR and TMR suggest that a spin contribution may get involved in, since it is the isotropic spin scattering instead of the anisotropic orbital scattering that mostly contributes to the LMR. It is worth to mention that the LMR is only about 10% of the TMR for the $x = 0.12$ sample, while it is about 60% for the $x = 0.15$ sample. Such an increasing component of spin-related MR suggests that the spin scattering is enhanced by Bi substitutions [25], and finally dominates in the positive TMR of $x \geqslant 0.31$ compounds [see Figs. 4(h) and 4(i)]. If the spin-orbit coupling is weak enough, the orbital contribution to MR (OMR) could be obtained by subtracting the LMR from the TMR. Then we have two kinds of OMR with opposite sign representing totally different orbital scattering mechanisms between $x = 0.12$ and 0.15 compounds. Indeed, it is further confirmed by the angular dependence of MR (AMR) shown in Fig. 6. Here, AMR is defined as

$$\Delta\rho_{ab}(\theta)/\rho_{ab} = [\rho_{ab}(\theta) - \rho_{ab}(0^\circ)]/\rho_{ab}(0^\circ), \qquad (4)$$

where the starting position $\theta = 0^\circ$ is corresponding to $H\|c$ geometry. A $\gamma \sin^2\theta$ dependence of positive AMR is found up to 50 K, the ending temperature of the upturn in $\rho_{ab}(T)$ for $x = 0.15$ [see Fig. 6(b)]. The AMR for $x = 0.12$ is negative and it also has $\sin^2\theta$ dependence except for $T = 12$ K. It is argued that such sharply increased magnitude of AMR [red points in Fig. 6(b)] might come from the suppression of a flux-flow dissipative process when the field became parallel to the ab plane [47,48], as shown by the dashed line in Fig. 6(a). Because the Nernst experiments [51] have already shown evidences of vortex above T_c but below the pseudogap opening temperature T^*, it is possible that the vortex dissipation introduces a linear-H contribution to TMR [see Fig. 5(b)] and a sharp dip in AMR [see Fig. 6(a)] of the slightly underdoped samples.

In WL theory [35,41], the negative OMR in the upturn region could be described as $\Delta\rho_{ab}^{\rm orb}/\rho_{ab} = -(H/H_e)^2$, where H_e is the characteristic field for elastic scattering. The elastic scattering length could be estimated by $L_e = (\hbar/4eH_e)^{1/2}$. Using the data in Figs. 5(c) and 5(d) [$(H/H_e)^2 = 0.35\%$ at $H = 9$ T and $T = 8$ K], we obtained $L_e = 10$ Å for $x = 0.15$, only twice the length of the in-plane lattice constants ($a \approx b \approx 5.3$ Å in orthorhombic unit cell). Furthermore, the transport mean free path $L_{\rm tr}$ could be estimated from the resistivity ρ_{ab} and the Hall coefficient R_H by the following equations based

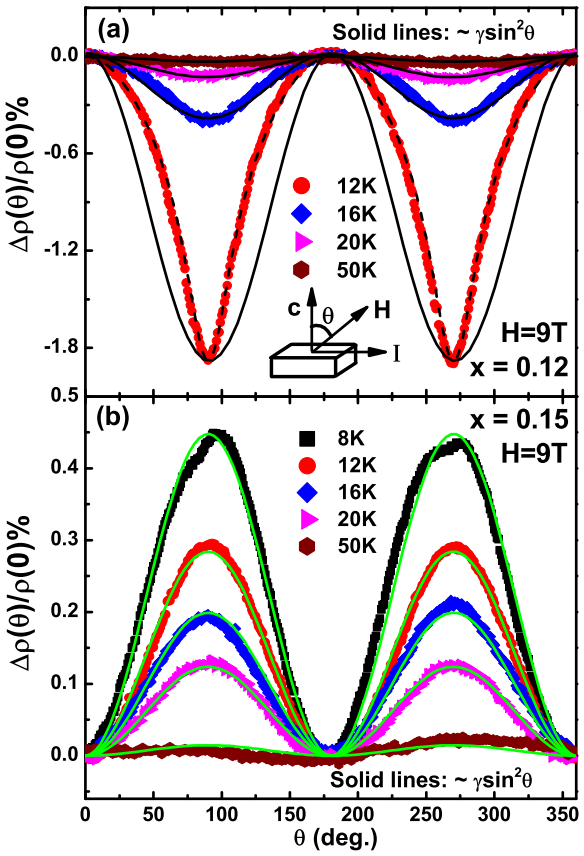

FIG. 6. (Color online) The angular dependence of MR in Bi2201 with (a) $x = 0.12$ and (b) $x = 0.15$ at 8, 12, 16, 20, and 50 K, where the solid lines are fitting results for $\sin^2\theta$ dependence, and dashed line is fitting data that involved both quasiparticle and flux-flow contributions [47,48].

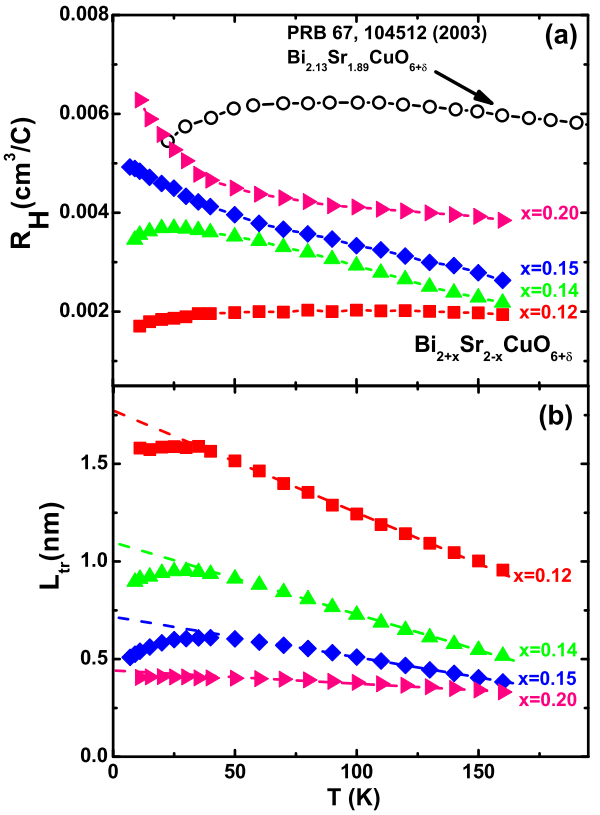

FIG. 7. (Color online) (a) Temperature dependence of Hall coefficient for $x = 0.12, 0.14, 0.15$, and 0.20. For comparison, we also plot the published data of $Bi_{2.13}Sr_{1.89}CuO_{6+\delta}$ [34], with a slight difference coming from the oxidation during growth process. (b) Temperature dependence of transport mean free path L_{tr} for $x = 0.12$, 0.14, 0.15, and 0.20, where the dashed lines are linear extrapolation above 30 K.

on 2D Fermi surface [27,52]:

$$\begin{cases} k_F^2 = \pi c/eR_H, \\ k_F L_{tr} = (h/e^2)/(2\rho_{ab}/c), \end{cases} \quad (5)$$

where $c = 24.6$ Å is the c-axis lattice constant, k_F is the Fermi wave vector, and h/e^2 is the natural unit for conductance. Figure 7(a) shows the temperature dependence of Hall coefficient R_H for our Bi2201 samples with $x = 0.12$, 0.14, 0.15, and 0.20, while Fig. 7(b) gives the transport mean free path L_{tr} deduced by the data from Figs. 7(a) and 2(a). From the linear temperature dependence of L_{tr} above 30 K, we can simply linearly extrapolate the data to $T = 0$ K and obtain $L_{tr}(0) = 18$, 11, 7, and 4 Å for $x = 0.12$, 0.14, 0.15, and 0.20, respectively. For reference, we also list the estimated data at $T = 50$ K in Table II, where $L_{tr}(0) = 15$, 9, 6, and 4 Å for $x = 0.12$, 0.14, 0.15, and 0.20, respectively. Although we should be careful for such estimation, since the concept of mean free path and of residual resistivity may be no longer valid when localization effects are important at low temperature, we still notice that the elastic scattering length L_e deduced from OMR is comparable with the transport mean free path L_{tr}. Again, the decreasing magnitude of mean free path indicates that the localization effect of charge carriers become stronger upon Bi substitution.

It should be noted that the previous results of x-ray diffraction on our Bi2201 crystals [9] suggest a contraction of c axis from $x = 0.20$ to 0.31, corresponding with the crossover regime from WL to SL as well as the disappearance of superconductivity in extremely underdoped regime (see Fig. 1). Such subtle change of crystal structure upon Bi substitution may change the electronic structure and further induce localization effects. In the out-of-plane substituted cuprates, the distance between the apical oxygen and Cu-O plane is stretched and the Cu-O cage is tilted [53]. The results of high-resolution transmission electron microscopy (TEM) on our Bi2201 crystals also suggest the distance between the Bi-concentrated regions increases upon Bi substitution, and thus we establish the relation between the structural

TABLE II. Estimated transport mean free path at $T = 50$ K for Bi2201 with $x = 0.12$, 0.14, 0.15, and 0.20.

x	R_H (cm^3/C)	ρ_{ab} (mΩ cm)	k_F (cm^{-1})	L_{tr} (Å)
0.12	0.00198	0.424	4.94×10^7	15
0.14	0.00352	0.940	3.70×10^7	9
0.15	0.00396	1.507	3.49×10^7	6
0.20	0.00450	2.408	3.27×10^7	4

modulation and the superconductivity [54]. Since the Cu-O planes take the main responsibility for conducting carriers, the dual effects both from the distortion between Cu-O planes and the reduction of p may reduce the bandwidth of electrons and cause localization effects [55]. This conclusion is further supported by recent scanning tunneling microscopy (STM) results, which show the electron structure changes on nanometre length scales in the Bi-based copper-oxide superconductors [6,56,57]. While in the high-purity Y123 crystals without out-of-plane substitution, thermal conductivity experiments found the delocalized fermionic excitations at zero energy in the nonsuperconducting state [58]. From another perspective, our results show the transport evidences on the localization effects induced by the out-of-plane substitutions in Bi2201 system.

IV. CONCLUSIONS

In summary, we established a localization picture of charge carriers in underdoped Bi2201 system. Upon out-of-plane Bi substitutions, the dual effects from the reduction of hole density and the subtle change of crystal structure give rise to a crossover from weak to strong localization, which push the system to the superconducting-insulating zone boundary and thus significantly suppress the superconductivity. Further research on the mechanism of localization and its detailed relation between superconductivity needs to be carried out by local probes such as STM, nuclear magnetic resonance, etc. The refinement from x-ray/neutron diffraction on single crystals will also be much helpful.

ACKNOWLEDGMENTS

This work is supported by the National Science Foundation of China, the Ministry of Science and Technology of China (973 project No. 2011CBA00110). The authors thank the fruitful discussion with Cong Ren, Hong Ding, Lei Shan, Ziqiang Wang, Shiliang Li, and Pengcheng Dai, and the great help on the crystal growth from Lei Fang, Peng Cheng, and Gang Mu.

[1] P. A. Lee, N. Nagaosa, and X. G. Wen, Rev. Mod. Phys. **78**, 17 (2006).
[2] J. Chang *et al.*, Nat. Phys. **8**, 871 (2012).
[3] Y. Y. Peng *et al.*, Nat. Commun. **4**, 2459 (2013).
[4] H. Eisaki, N. Kaneko, D. L. Feng, A. Damascelli, P. K. Mang, K. M. Shen, Z.-X. Shen, and M. Greven, Phys. Rev. B **69**, 064512 (2004).
[5] K. Fujita, T. Noda, K. M. Kojima, H. Eisaki, and S. Uchida, Phys. Rev. Lett. **95**, 097006 (2005).
[6] J. A. Slezak *et al.*, Proc. Natl. Acad. Sci. USA **105**, 3203 (2008).
[7] S. I. Vedeneev, A. G. M. Jansen, E. Haanappel, and P. Wyder, Phys. Rev. B **60**, 12467 (1999).
[8] S. I. Vedeneev, Cyril Proust, V. P. Mineev, M. Nardone, and G. L. J. A. Rikken, Phys. Rev. B **73**, 014528 (2006).
[9] H.-Q. Luo, L. Fang, G. Mu, and H.-H. Wen, J. Crystal Growth **305**, 222 (2007).
[10] H.-Q. Luo, P. Cheng, L. Fang, and H.-H. Wen, Supercond. Sci. Technol. **21**, 125024 (2008).
[11] H.-H. Wen, G. Mu, H.-Q. Luo, H. Yang, L. Shan, C. Ren, P. Cheng, J. Yan, and L. Fang, Phys. Rev. Lett. **103**, 067002 (2009).
[12] Y. Ando, G. S. Boebinger, A. Passner, T. Kimura, and K. Kishio, Phys. Rev. Lett. **75**, 4662 (1995).
[13] Y. Ando, G. S. Boebinger, A. Passner, N. L. Wang, C. Geibel, and F. Steglich, Phys. Rev. Lett. **77**, 2065 (1996).
[14] Y. Ando *et al.*, Physica C **282–287**, 240 (1997).
[15] Y. Ando, G. S. Boebinger, A. Passner, N. L. Wang, C. Geibel, F. Steglich, I. E. Trofimov, and F. F. Balakirev, Phys. Rev. B **56**, R8530 (1997).
[16] Y. Ando, Y. Hanaki, S. Ono, T. Murayama, K. Segawa, N. Miyamoto, and S. Komiya, Phys. Rev. B **61**, R14956 (2000).
[17] S. Ono, Y. Ando, T. Murayama, F. F. Balakirev, J. B. Betts, and G. S. Boebinger, Phys. Rev. Lett. **85**, 638 (2000).
[18] S. I. Vedeneev and D. K. Maude, Phys. Rev. B **70**, 184524 (2004).
[19] S. I. Vedeneev, A. G. M. Jansen, and P. Wyder, Phys. Rev. B **62**, 5997 (2000).
[20] C. Proust, K. Behnia, R. Bel, D. Maude, and S. I. Vedeneev, Phys. Rev. B **72**, 214511 (2005).
[21] S. I. Vedeneev, Physics-Uspekhi **55**, 625 (2012).
[22] S. I. Vedeneev and Y. N. Ovchinnikov, JETP. Lett. **75**, 195 (2002).
[23] S. I. Vedeneev, A. G. M. Jansen, and P. Wyder, JETP. **90**, 1042 (2000).
[24] S. I. Vedeneev, D. K. Maude, E. Haanappel, and V. P. Mineev, Phys. Rev. B **75**, 064512 (2007).
[25] F. Rullier-Albenque, H. Alloul, and R. Tourbot, Phys. Rev. Lett. **87**, 157001 (2001).
[26] F. Rullier-Albenque, H. Alloul, F. Balakirev, and C. Proust, Europhys. Lett. **81**, 37008 (2008).
[27] T. W. Jing, N. P. Ong, T. V. Ramakrishnan, J. M. Tarascon, and K. Remschnig, Phys. Rev. Lett. **67**, 761 (1991).
[28] M.-Y. Choi and J. S. Kim, Phys. Rev. B **61**, 11321 (2000).
[29] K. Kudo, N. Okumura, Y. Miyoshi, T. Nishizaki, T. Sasaki, and N. Kobayashi, J. Phys. Soc. Jap. **78**, 084722 (2009).
[30] J. L. Tallon, C. Bernhard, H. Shaked, R. L. Hitterman, and J. D. Jorgensen, Phys. Rev. B **51**, 12911 (1995).
[31] M. R. Presland, J. L. Tallon, R. Buckley, R. S. Liu, and N. Flower, Physica C **176**, 95 (1991).
[32] Z.-H. Pan *et al.*, Phys. Rev. B **79**, 092507 (2009).
[33] C. C. Torardi, M. A. Subramanian, J. C. Calabrese, J. Gopalakrishnan, E. M. McCarron, K. J. Morrissey, T. R. Askew, R. B. Flippen, U. Chowdhry, and A. W. Sleight, Phys. Rev. B **38**, 225 (1988).
[34] S. Ono and Y. Ando, Phys. Rev. B **67**, 104512 (2003).
[35] P. A. Lee and T. V. Ramakrishnan, Rev. Mod. Phys. **57**, 287 (1985).
[36] C. Y. Chen, E. C. Branlund, C. S. Bae, K. Yang, M. A. Kastner, A. Cassanho, and R. J. Birgeneau, Phys. Rev. B **51**, 3671 (1995).
[37] N. W. Preyer, M. A. Kastner, C. Y. Chen, and R. J. Birgeneau, Y. Hidaka, Phys. Rev. B **44**, 407 (1991).

[38] A. L. Efros, J. Phys. C: Solid State Phys. **9**, 2021 (1976).
[39] V. I. Kozub, A. A. Zyuzin, Y. M. Galperin, and V. Vinokur, Phys. Rev. Lett. **96**, 107004 (2006).
[40] S. Salem-Sugui, Jr, A. D. Alvarenga, J. Mosqueira, J. D. Dancausa, C. Salazar Mejia, E. Sinnecker, H.-Q. Luo, and H.-H. Wen, Supercond. Sci. Technol. **25**, 105004 (2012).
[41] G. Bergman, Phys. Rev. Lett. **48**, 1046 (1982).
[42] E. Cimpoiasu, G. A. Levin, C. C. Almasan, A. P. Paulikas, and B. W. Veal, Phys. Rev. B **64**, 104514 (2001).
[43] M. Z. Cieplak, A. Malinowski, S. Guha, and M. Berkowski, Phys. Rev. Lett. **92**, 187003 (2004).
[44] A. N. Lavrov, Y. Ando, and S. Ono, Physica C **341–348**, 1579 (2000).
[45] M. Enoki, M. Fujita, T. Nishizaki, S. Iikubo, D. K. Singh, S. Chang, J. M. Tranquada, and K. Yamada, Phys. Rev. Lett. **110**, 017004 (2013).
[46] T. Kimura, S. Miyasaka, H. Takagi, K. Tamasaku, H. Eisaki, S. Uchida, K. Kitazawa, M. Hiroi, M. Sera, and N. Kobayashi, Phys. Rev. B **53**, 8733 (1996).
[47] V. Sandu, E. Cimpoiasu, T. Katuwal, S. Li, M. B. Maple, and C. C. Almasan, Phys. Rev. Lett. **93**, 177005 (2004).
[48] T. Katuwal, V. Sandu, C. C. Almasan, B. J. Taylor, and M. B. Maple, Phys. Rev. B **72**, 174501 (2005).
[49] J. M. Harris, Y. F. Yan, P. Matl, N. P. Ong, P. W. Anderson, T. Kimura, and K. Kitazawa, Phys. Rev. Lett. **75**, 1391 (1995).
[50] H. J. Kim, P. Chowdhury, S. K. Gupta, N. H. Dan, and S. I. Lee, Phys. Rev. B **70**, 144510 (2004).
[51] Y. Wang, Z. A. Xu, T. Kakeshita, S. Uchida, S. Ono, Yoichi Ando, and N. P. Ong, Phys. Rev. B **64**, 224519 (2001).
[52] S. J. Hagen, T. W. Jing, Z. Z. Wang, J. Horvath, and N. P. Ong, Phys. Rev. B **37**, 7928 (1988).
[53] D. Grebille, H. Leligny, A. Ruyter, P. H. Labbe, and B. Raveau, Acta Crystallogr. B **52**, 628 (1996).
[54] X. M. Li, F. H. Li, H.-Q. Luo, L. Fang, and H.-H. Wen, Supercond. Sci. Technol. **22**, 065003 (2009).
[55] A. T. Fiory, S. Martin, R. M. Fleming, L. F. Schneemeyer, and J. V. Waszczak, Phys. Rev. B **41**, 2627 (1990).
[56] W. D. Wise *et al*., Nat. Phys. **5**, 213 (2009).
[57] Y. Kohsaka *et al*., Nature (London) **454**, 1072 (2008).
[58] M. Sutherland *et al*., Phys. Rev. Lett. **94**, 147004 (2005).